ACOUSTOELECTROCHEMISTRY: THE APPLICATION OF SOUND TO ELECTROCHEMICAL PROCESSES

DG Offin School of Chemistry, University of Southampton, Southampton, SO17 1BJ, UK
PR Birkin School of Chemistry, University of Southampton, Southampton, SO17 1BJ, UK
TG Leighton ISVR, University of Southampton, Southampton, SO17 1BJ, UK
PF Joseph ISVR, University of Southampton, Southampton, SO17 1BJ, UK

1 INTRODUCTION

The interaction of sound and bubbles is well known in acoustics[1]. However, in electrochemistry, a field in which bubbles can play important roles, it is rarely considered. In this work the interaction of sound and bubbles has been investigated as a tool for enhancing mass transfer in electrochemical processes. Often the rate of electrochemical processes is limited by the rate of mass transfer of electroactive species to the electrode surface. There exist a number of strategies, which are designed to increase fluid motion in electrochemical cells. It is well known that the introduction of bubbles into an electrochemical cell can enhance fluid mixing[2-6]. For example, in industrial electrochemical processes, gas sparging has been studied for many years as a technique for enhancing current densities[7-13]. Other techniques designed to enhance mass transfer include turbulence promoters[14, 15], high velocity electrolyte pumping, and electrode vibration[16]. Ultrasound has also been used to generate high rates of mass transfer[17-21]. Through the use of piston-like emitters operated at frequencies of ~20 kHz, high levels of acoustic streaming can be generated, together with both inertial and non-inertial cavitation. This leads to extremely high mass transfer coefficients (0.1 - 1 cm s^{-1}). However, this is highly energy intensive compared to small amplitude bubble oscillation. It is known that driving pressure fields in excess of 100 kPa are required to generate inertial cavitation (under continuous sound irradiation in water and normal temperature and pressure conditions[22, 23]). Also, the presence of inertial cavitation events can lead to erosion of the electrode surface[24-26]. This may not be a problem for electroanalytical techniques but is severely limiting if the technology is to be employed in processes such as electrowinning or electroplating. In an alternative approach, targeted bubble oscillation has been used to achieve relatively high rates of mass transfer[27, 28]. In this technique large (~ 2 millimetre radius), tethered gas bubbles were driven to oscillation by a tuneable sound field. By targeting bubble resonance and the excitation of surface waves, low amplitude driving fields (~100 Pa) can be used to generate mass transfer coefficients of up to 0.05 cm s^{-1}. While this is an order of magnitude less than the mass transfer coefficients achievable through the use of ultrasound, the driving pressures required are 10^3 times lower and in turn the intensity is 10^6 times less[27]. The aim of the work presented here was to assess the use of targeted bubble oscillation in rising bubble systems as opposed to the tethered bubbles previously investigated[27, 28]. In this work a single bubble stream was used, which represents the first stage of a stepwise investigation into the use of acoustic excitation as a tool for mass transfer enhancement in multibubble electrochemical reactors.

2 EXPERIMENTAL

For all electrochemical experiments a two electrode setup was employed. A silver wire acted as the reference/counter electrode and a potentiostat built in-house was used. The output from the potentiostat was recorded *via* a PC and ADC card (National Instruments PCI-60205E). In order to reduce electrical noise a Faraday cage was employed at all times. Cyclic voltammetry was recorded in a glass cell fitted with a water jacket in order to control the temperature of the solution. The temperature was maintained at 25 °C and aerobic conditions were used. All acoustoelectrochemical experiments were carried out in a specially designed cell (see Figure 1a). The body of the cell was a glass tube (diameter 47 mm), modified to include a flat window and an arm terminated with an SQ13 joint. A Mylar speaker (47 mm diameter, 0.2 W, Maplin Electronics), which had its contacts insulated from the solution[28], was glued to the bottom of the tube with fast

setting epoxy resin (RS). The speaker was driven by a function generator (Thurlby Thandar TGA 12101) and amplifier (HH Electronics TPA-50D). Argon gas (Pureshield, BOC) was injected by means of a 19G (0.7 mm i.d.) needle, which was screwed onto the SQ 13 joint. The flow rate of the gas (see appropriate figure legends) was controlled using a mass flow controller (Bronkhorst F-200CV). For acoustoelectrochemical experiments the temperature of the solution was not controlled. The embedded Pt working electrode (see Figure 1b) was made as follows. First, the tip of a glass Pasteur pipette was heated in a flame, bent to a 90° angle and allowed to cool. A 2 cm length of Pt wire (50 µm diameter, 99.99%, Goodfellow) was soldered to a length of multicore copper wire and carefully threaded through the Pasteur pipette. The pipette was then filled with slow setting epoxy resin (Epofix, Struers) and allowed to cure overnight. Second, a hole (1 mm diameter) was drilled in the centre of a 40 mm × 15 mm copper plate (2 mm thickness). The end of the Pasteur pipette was positioned through the hole and glued into place with fast setting epoxy resin. Third, the face of the copper plate was polished flat with increasing grades of silicon carbide paper (up to 1200) and an aqueous alumina slurry (1 µm). The working electrode was positioned in the cell by means of a computer controlled XYZ scanning rig (Zaber T-LA60A linear actuators and TSB60 translation stages) such that the bubble stream was aligned with the microelectrode. All solutions were made up using water from a USF Elga Purelab Option E10 purification system. Water purified in this manner had a conductivity of below 0.1 µS cm^{-1} and a low organic content (manufacture's quoted TOC < 30 ppb). Strontium nitrate (99+ %, Aldrich) and potassium ferricyanide (99.5%, Aldrich) were used as received. All pressure measurements were made in the centre of the cell in the absence of the electrode (due to space constraints) and bubble injection using a G.R.A.S. 10CT hydrophone.

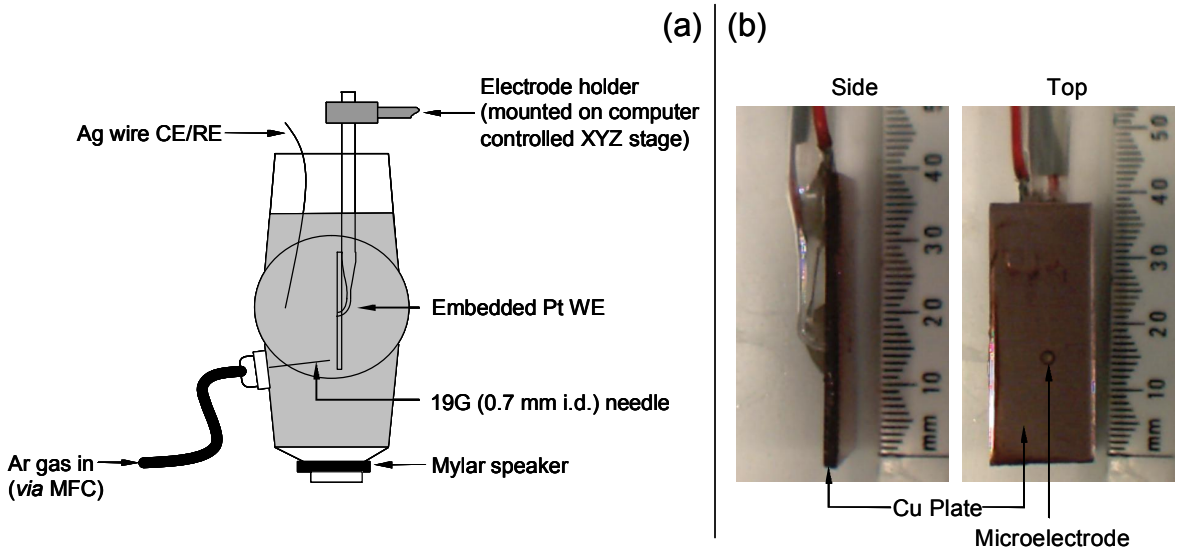

Figure 1a. Experimental setup. b. Side and top views of the embedded 50 µm diameter Pt microeletrode.

3 RESULTS AND DISCUSSION

The effect of bubble injection and insonification were assessed using an embedded Pt microelectrode (see Experimental section). The copper plate served to approximate a large electrode (as might be employed in an electrochemical reactor), while the use of a microelectrode allowed local mass transfer effects to be probed under steady state conditions. The microelectrode samples a small volume of solution and also benefits from fast response times allowing the effects of individual bubbles to be detected. Prior to assessing the effect of bubble injection and insonification however, it is important to characterise the electrochemical response of the microelectrode in the test solution. The electrolyte used was 5 mM $K_3Fe(CN)_6$ and 0.1 M $Sr(NO_3)_2$ to which 50 % (by weight) sucrose was added. The addition of sucrose increased the viscosity of

the solution by approximately 3.5 times[29], such that the path of the rising bubbles was found to be more reproducible. Figure 2 shows a cyclic voltammogram recorded using a 25 μm diameter platinum microelectrode in the test solution. The scan was started at +0.4 V *vs.* Ag and swept to -0.1 V *vs.* Ag and back at a sweep rate of 5 mV s^{-1}. The form of the voltammogram is a characteristic sigmoidal curve due to the electro-reduction of $Fe(CN)_6^{3-}$ at the electrode surface and the mass transfer characteristics of microelectrodes under steady state conditions. A clear plateau exists from 0 V *vs.* Ag to -0.1 V *vs.* Ag, which corresponds to the mass transfer limited reduction of the $Fe(CN)_6^{3-}$ species. The mass transfer limited current was found to be -4.8 nA. This corresponds to a mass transfer coefficient of 0.002 cm s^{-1}, or a diffusion coefficient for $Fe(CN)_6^{3-}$ of 2.03×10^{-6} cm^2 s^{-1}. This is in good agreement with the literature value[30] of 7.26×10^{-6} cm^2 s^{-1} (measured in 1 M KCl) considering the increased viscosity of the solution employed here and the inverse proportionality between viscosity and diffusion coefficient predicted by the Stokes-Einstein relationship.

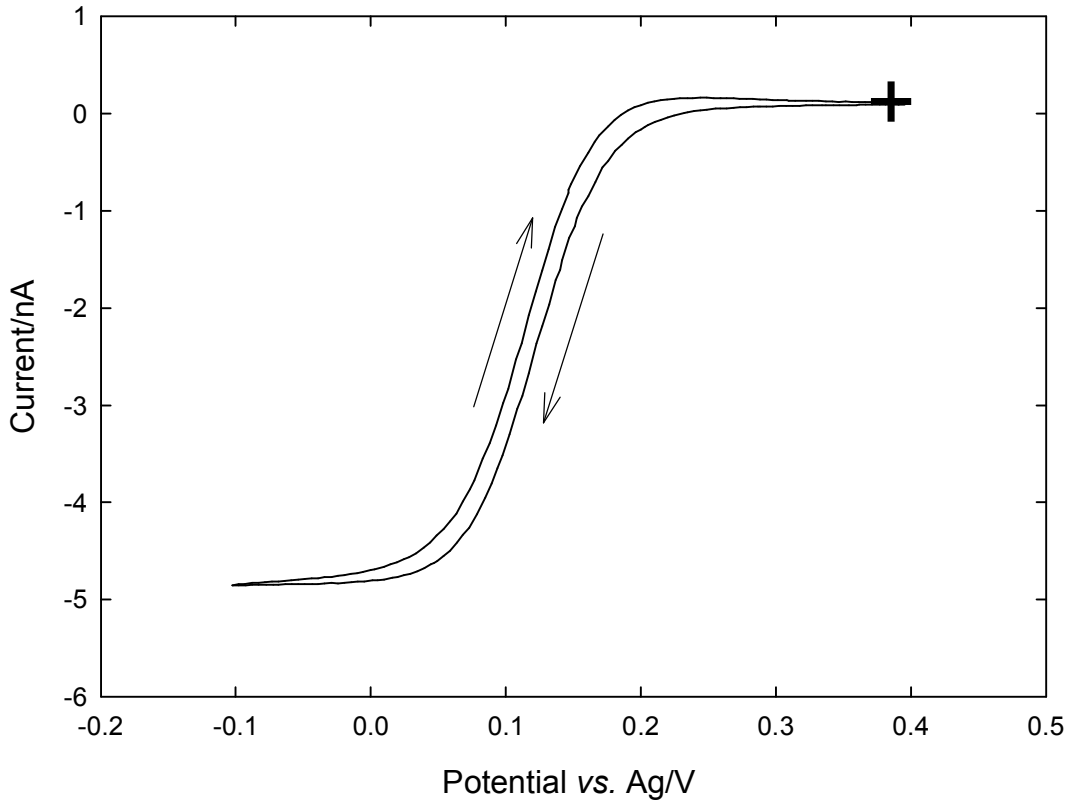

Figure 2. Cyclic voltammogram recorded at a 25 μm diameter Pt microelectrode in a solution of 5 mM $K_3Fe(CN)_6$ and 0.1 M $Sr(NO_3)_2$ to which 50 % (by weight) sucrose was added. The plus symbol (**+**) indicates the start position and the arrows indicate the direction of the scans. The scan rate was 5 mV s^{-1}. The experiment was carried out at 25 °C and under aerobic conditions.

Following electrochemical characterisation, the effects of bubble injection and insonification were assessed. Figure 3 shows the current recorded at an embedded Pt microelectrode (50 μm diameter) in a solution of 5 mM $K_3Fe(CN)_6$ and 0.1 M $Sr(NO_3)_2$ to which 50 % (by weight) sucrose was added under various experimental conditions. At all times the potential of the microelectrode was held at -0.1 V *vs.* Ag, which ensured mass transfer limited reduction of $Fe(CN)_6^{3-}$ (see Figure 2). Initially the electrode was in the solution in the absence of any bubbles or insonification and a current of -9.6 nA was observed. This is twice the mass transfer limited current seen in Figure 2 because the electrode used here is twice the radius of that used in Figure 2 (for microelectrodes the limiting current scales linearly with electrode radius). After approximately 10 seconds the gas flow was turned on and the cathodic current can be seen to increase to –20.7 nA, slightly more than

twice the current observed under silent, bubble-free conditions. There is some delay in the enhancement because of the time taken for the gas flow to reach the maximum rate. The enhanced current, which was observed, is indicative of forced convection in the cell distorting the diffusion hemisphere at the platinum electrode leading to an enhanced reduction current. The enhancement is uniform, which is to be expected as the centre of the bubble stream is 2.7 mm from the electrode surface. Given the radius of the bubbles is 1.1 ± 0.1 mm (see Figure 4), the edge of the bubble stream is at least 1.5 mm from the electrode. Whitney and Tobias[6] have shown that a stream of bubbles and entrained liquid rising outside the diffusion layer of an electrode can be treated as an equivalent cylinder rising with the same drag coefficient. This results in a uniform current enhancement, as observed here. At a time of 30 s sound was turned on at 2.86 kHz. The bubble stream was seen to be attracted towards the copper plate and rise up the plate in contact with the surface. The choice of frequency was determined by observation of the bubble stream while the frequency was swept from 2 kHz to 4 kHz. The frequency which gave the greatest translation of the bubble stream was used. The translation of the rising bubbles can be seen in Figures 4a and b, which show photographs taken in the absence and presence of sound respectively. In Figure 4a, a bubble can be seen at a distance (to the bubble centre) of 2.7 mm from the copper plate, which is the dark area at the right of each picture. In Figure 4b however, it can be seen that a similar bubble, in the presence of insonification at 2.86 kHz, rises in contact with the copper plate. All other conditions are identical.

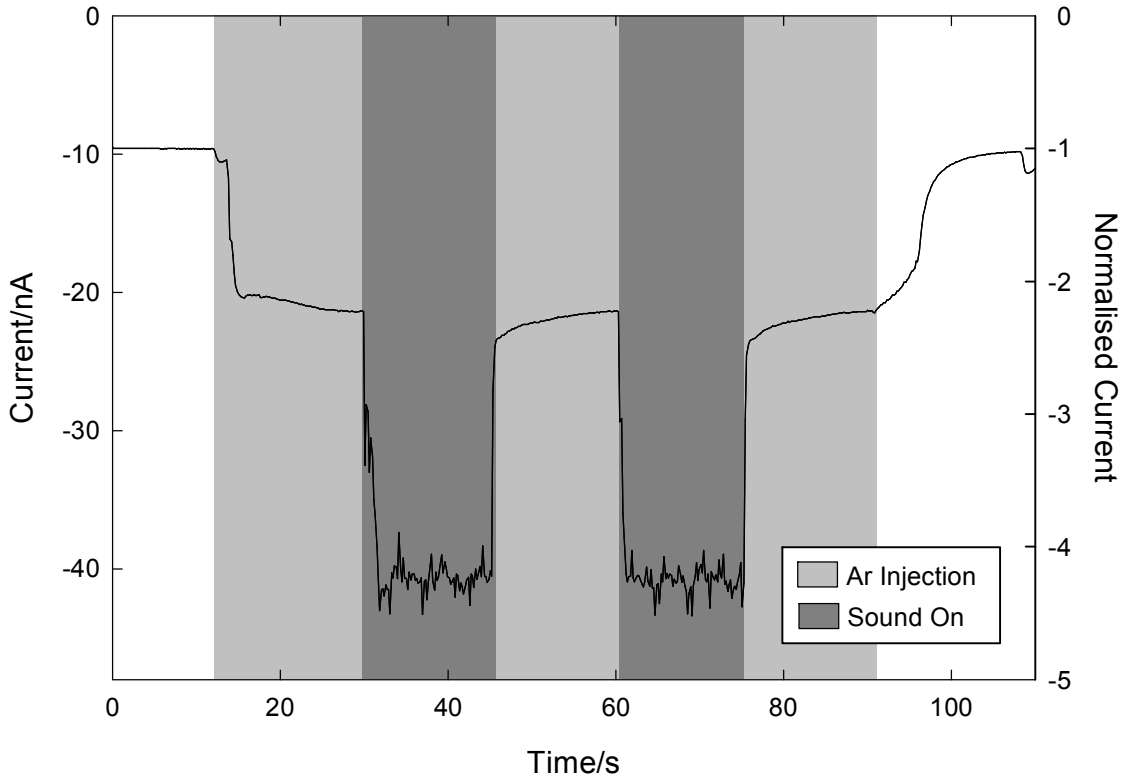

Figure 3. Plot showing the current recorded at a 50 μm embedded Pt electrode as a function of time under various experimental conditions. The normalised current refers to the current recorded in the absence of sound and Ar injection. The electrolyte was a solution of 5 mM $K_3Fe(CN)_6$ and 0.1 M $Sr(NO_3)_2$ to which 50 % (by weight) sucrose was added. The Ar injection rate was 2 mL min^{-1}. The sound frequency was 2.86 kHz. The pressure amplitude measured in the centre of the cell in the absence of the electrode and bubble injection was 322 Pa. The distance between the centre of the bubble stream and the copper plate was 2.7 mm.

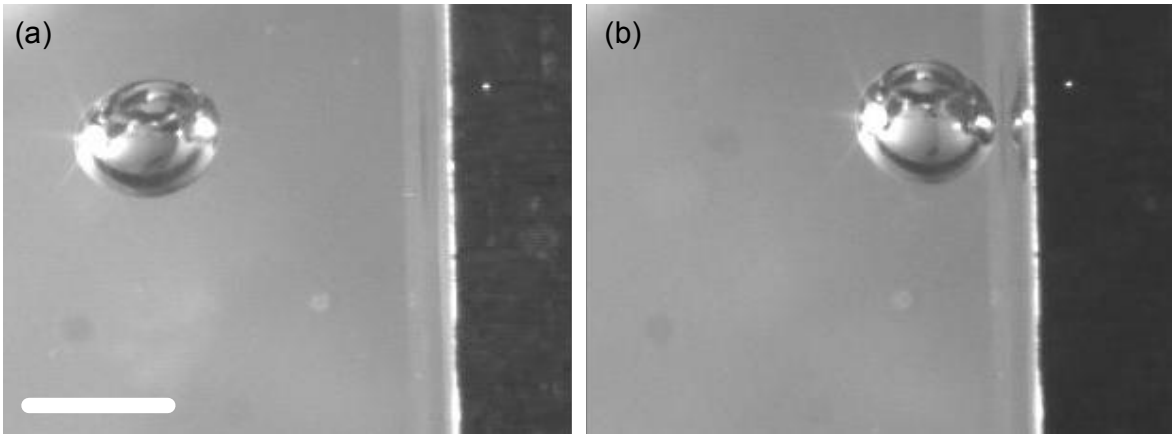

Figure 4. Photographs of rising bubbles in the absence (a) and presence (b) of insonification at 2.86 kHz. The pressure amplitude measured in the centre of the cell in the absence of the electrode and bubble injection was 322 Pa. In both cases all other conditions are identical. The dark area at the right of each frame is a copper plate. The scale bar in (a) represents 2 mm.

Figure 3 shows that the current measured at the platinum microelectrode under insonification was more than 4 times the current observed under silent, bubble-free conditions. Unlike the current enhancement seen in the presence of the bubble stream alone, the enhancement is not uniform with time and appears 'noisy'. After 45 s the sound was turned off. The bubble stream was seen to return to its original position and the current fell to a value similar to that seen before insonification. In order to illustrate the reproducibility of the effect the sound was turned on again after 60 s. The bubbles were observed to be attracted to the copper plate as before and a similar current enhancement was seen. After the sound was turned off for the second time (at 75 s) the current again decreased. The gas flow was then turned off and the current decayed back to that seen at the start of the experiment. As with the commencement of gas injection, there is a delay in the current decrease caused by the time required for the gas flow to stop.

In order to investigate the effect of the combined gas injection and insonification further, the current was recorded at much higher temporal resolution. This is shown in Figure 5. It can be seen that the current enhancement consists of periodic, transient increases, which are up to 5.5 times the silent, bubble-free current. The transient current increases are attributed to the disruption of the diffusion hemisphere at the platinum electrode by individual bubbles, which rise up the copper plate in contact with the surface. This observation is also in agreement with the work of Whitney and Tobias[6].

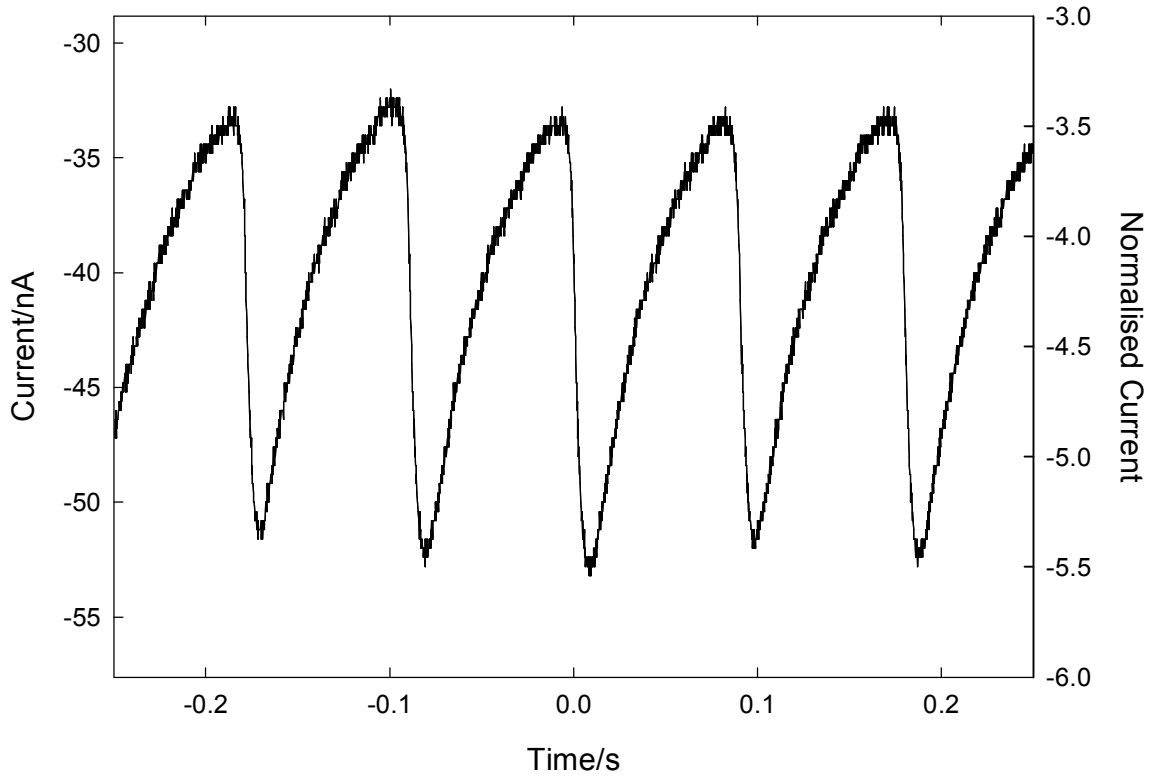

Figure 5. Plot showing the current recorded at a 50 µm embedded Pt electrode as a function of time in the presence of Ar injection and insonification. The normalised current refers to the current recorded in the absence of sound and Ar injection. The electrolyte was a solution of 5 mM $K_3Fe(CN)_6$ and 0.1 M $Sr(NO_3)_2$ to which 50 % (by weight) sucrose was added. The Ar injection rate was 2 mL min^{-1}. The sound frequency was 2.86 kHz. The pressure amplitude measured in the centre of the cell in the absence of the electrode and bubble injection was 322 Pa. The distance between the centre of the bubble stream and the copper plate was 2.7 mm.

The exact nature of the attractive force, which acts between the bubbles and the copper plate under insonification, is currently under investigation. However, presently it assumed that both primary and secondary Bjerknes forces will act on the oscillating bubble within the cell close to the solid/liquid boundary represented by the copper plate. Given the bubbles have radii of 1.1 ± 0.1 mm (see Figure 4), the Minnaert resonance frequency is expected to be 2590 – 3100 Hz. The excitation frequency employed here was 2.86 kHz. It is therefore expected that the rising bubble will undergo relatively large volume pulsations. It is well known that bubbles oscillating in this fashion are attracted to rigid boundaries[31]. However, the pressure amplitude measured in the centre of the cell in the absence of the electrode (due to space constraints) was 322 Pa. This is sufficient to excite multiple surface wave modes at the gas liquid interface of the rising bubbles[28, 32]. However, figure 4 shows that clear surface wave oscillations where not observed. This may be due to the local conditions at the solid/liquid boundary. Hence, the exact mechanisms involved in the generation of enhanced mass transfer in the presence of dual excitation (bubble buoyancy and sound irradiation) are unclear at this time and under further investigation.

In order to assess the distance dependence of the attractive force, the current at the 50 µm embedded Pt microelectrode was measured as a function of distance from the bubble stream in the presence of the bubble injection alone and in the presence of bubble injection coupled with insonification. The results of this are shown in Figure 6. The circles (●) show the average current recorded in the presence of the bubble stream alone and the triangles (▾) show the average current recorded in the presence of the bubble stream and insonification. It can be seen that in the

absence of insonification, as the electrode is moved away from the bubble stream, the current quickly falls. However, in the presence of insonification the enhancement is maintained to greater distances. For comparison it is helpful to consider the insert to Figure 6, which shows the current measured in the presence of insonification normalised to the current recorded in its absence. It can be seen that at small distances there is a small benefit produced by insonification (the normalised current is ~1.25). However, the greatest benefit is seen just below 3 mm, where the normalised current is more than 2. This corresponds to the greatest translation of the bubble stream toward the plate. Beyond this distance the normalised current falls dramatically. It was observed that at distances greater than 3 mm the bubbles were no longer attracted to the copper plate.

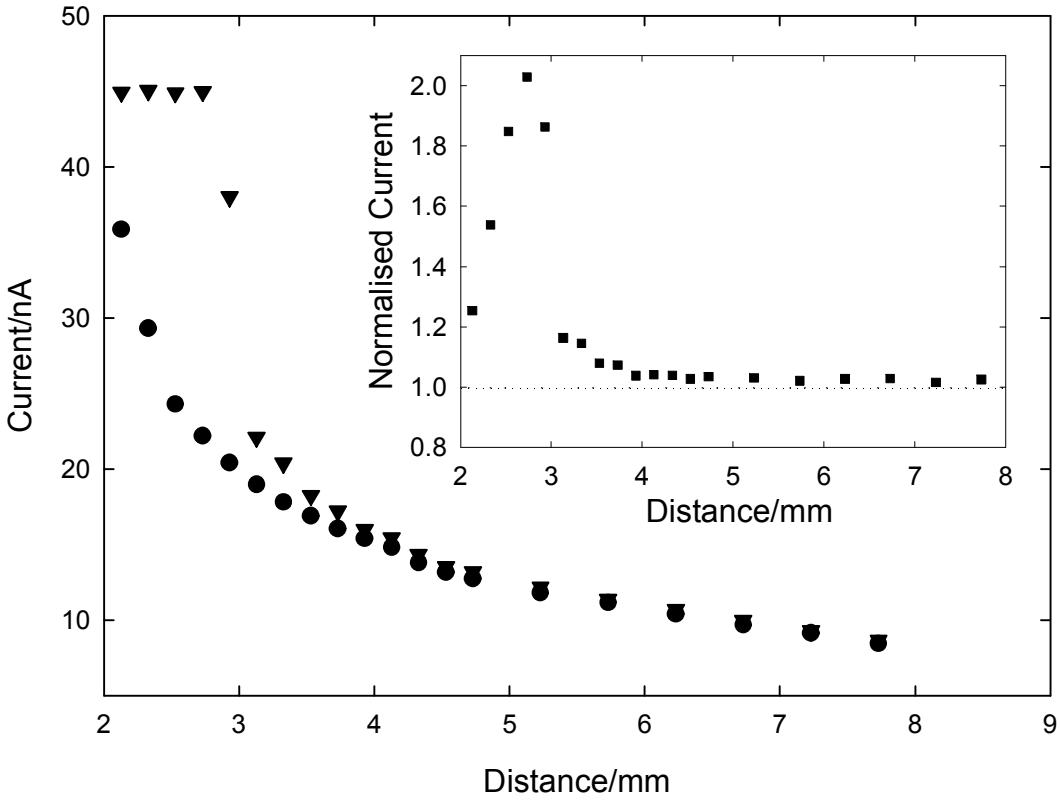

Figure 6. Plot showing the average current recorded at a 50 μm embedded Pt electrode as a function of distance between the copper plate and the centre of the bubble stream under various experimental conditions. The circles (●) represent the current recorded in the presence of gas injection alone. The triangles (▼) represent the current recorded in the presence of gas injection and insonification. The electrolyte was a solution of 5 mM $K_3Fe(CN)_6$ and 0.1 M $Sr(NO_3)_2$ to which 50 % (by weight) sucrose was added. The Ar injection rate was 2 mL min^{-1}. The sound frequency was 2.86 kHz. The pressure amplitude measured in the centre of the cell in the absence of the electrode and bubble injection was 322 Pa. The insert is a plot showing the average current recorded in the presence of gas injection and insonification normalised to the average current recorded in the presence of gas injection alone.

4 CONCLUSIONS

In this work a Pt microelectrode embedded in a copper plate has been used to assess the effect of bubble injection and insonification on the mass transfer in an electrochemical cell. The embedded electrode was used so as to approximate a large electrode in terms of construction, while allowing local mass transfer effects to be probed at high temporal resolution. It has been shown that the

introduction of bubbles into the cell leads to enhanced mass transfer due to forced convection. However, applying an appropriate sound field (tuned to the resonance frequency of the bubbles) caused the bubbles to become attracted to the rigid surface. This generated further gains in mass transfer and extended the range over which mass transfer enhancement was seen.

5 ACKNOWLEDGEMENTS

We gratefully acknowledge funding for this project provided by EPSRC under grant GR/S78698/01.

6 REFERENCES

1. T. G. Leighton, The Acoustic Bubble, Academic Press Limited, London (1994).
2. G. H. Sedahmed, M. S. Abdo, M. A. Kamal, O. A. Fadaly, H. M. Osman, 'Effect of gas sparging on the rate of mass transfer during electropolishing of vertical plates', Chem. Eng. Process., 40 (3), 195 (2001).
3. A. Shah, J. Jorne, 'Mass-Transfer Under Bubble-Induced Convection In A Vertical Electrochemical-Cell', J. Electrochem. Soc., 136 (1), 144 (1989).
4. W. S. Wu, G. P. Rangaiah, 'Effect Of Gas Evolution On Mass-Transfer In An Electrochemical Reactor', J. Appl. Electrochem., 23 (11), 1139 (1993).
5. G. M. Whitney, C. W. Tobias, 'Mass-Transfer Effects Of Bubble Streams Rising Past Vertical Electrodes', J. Electrochem. Soc., 134 (3), C133 (1987).
6. G. M. Whitney, C. W. Tobias, 'Mass-Transfer Effects Of Bubble Streams Rising Near Vertical Electrodes', AIChE Journal, 34 (12), 1981 (1988).
7. W. C. Cooper, 'Reviews Of Applied Electrochemistry 11. Advances And Future-Prospects In Copper Electrowinning', J. Appl. Electrochem., 15 (6), 789 (1985).
8. W. C. Cooper, K. K. Mishra, 'The Nature Of Copper Electrowon In The Presence Of Iron Using Sulfur-Dioxide Sparging', Hydrometallurgy, 17 (3), 305 (1987).
9. W. W. Harvey, M. R. Randlett, K. I. Bangerskis, 'Cell Design Components Of Ledgemont Air-Agitation Close-Spacing Methods Of High-Current Density Copper Electrowinning And Electrorefining', Chem. Ind., (9), 379 (1975).
10. W. W. Harvey, M. R. Randlett, K. I. Bangerskis, 'Exploratory Development Of Air-Agitation Copper Electrorefining', J. Metals, 30 (7), 32 (1978).
11. L. J. J. Janssen, J. G. Hoogland, 'Effect Of Electrolytically Evolved Gas Bubbles On Thickness Of Diffusion Layer', Electrochim. Acta, 15 (6), 1013 (1970).
12. D. A. Uceda, T. J. O'Keefe, 'Electrochemical Evaluation Of Copper Deposition With Gas Sparging', J. Appl. Electrochem., 20 (2), 327 (1990).
13. G. D. Rigby, P. E. Grazier, A. D. Stuart, E. P. Smithson, 'Gas bubble induced mixing in electrowinning baths', Chem. Eng. Sci., 56 (21-22), 6329 (2001).
14. V. D. Stankovic, 'Limiting Current-Density And Specific Energy-Consumption In Electrochemical-Cells With Inert Turbulence Promoters', J. Appl. Electrochem., 24 (6), 525 (1994).
15. T. Subbaiah, P. Venkateswarlu, S. C. Das, R. P. Das, G. Raju, 'Mass transfer conditions in an electrochemical cell in the presence of turbulence promoters', Plat. Surf. Finish., 86 (1), 94 (1999).
16. H. Gomaa, A. M. Al Taweel, J. Landau, 'Mass transfer enhancement at vibrating electrodes', Chem. Eng. J., 97 (2-3), 141 (2004).
17. P. R. Birkin, S. Silva-Martinez, 'A study of the effect of ultrasound on mass transport to a microelectrode', J. Electroanal. Chem., 416 127 (1996).
18. F. Marken, R. G. Compton, S. G. Davies, S. D. Bull, T. Thiemann, M. Melo, A. C. Neves, J. Castillo, C. G. Jung, A. Fontana, 'Electrolysis in the presence of ultrasound: cell geometries for the application of extreme rates of mass transfer in electrosynthesis', J. Chem. Soc.-Perkin Trans. 2, (10), 2055 (1997).
19. B. G. Pollet, J. P. Lorimer, J. Y. Hihn, S. S. Phull, T. J. Mason, D. J. Walton, 'The effect of ultrasound upon the oxidation of thiosulphate on stainless steel and platinum electrodes', Ultrason. Sonochem., 9 (5), 267 (2002).

20. J. Klima, C. Bernard, C. Degrand, 'Sonoelectrochemistry: transient cavitation in acetonitrile in the neighbourhood of a polarized electrode', J. Electroanal. Chem., 399 147 (1995).
21. F. Javier Del Campo, J. Melville, J. L. Hardcastle, R. G. Compton, 'Differential pulse and chronoamperometric studies of insonated systems: Acoustic streaming and cavitation effects', J. Phys. Chem. A, 105 666 (2001).
22. C. K. Holland, R. E. Apfel, 'An Improved Theory For The Prediction Of Microcavitation Thresholds', IEEE Trans. Ultrason. Ferroelectr. Freq. Control, 36 (2), 204 (1989).
23. P. R. Birkin, D. G. Offin, T. G. Leighton, 'Experimental and theoretical characterisation of sonochemical cells. Part 2: cell disruptors (Ultrasonic horns) and cavity cluster collapse', Phys. Chem. Chem. Phys., 7 (3), 530 (2005).
24. P. R. Birkin, D. G. Offin, T. G. Leighton, 'The study of surface processes under electrochemical control in the presence of inertial cavitation', Wear, 258 (1-4), 623 (2005).
25. P. R. Birkin, D. G. Offin, T. G. Leighton, 'Electrochemical measurements of the effects of inertial acoustic cavitation by means of a novel dual microelectrode', Electrochem. Commun., 6 (11), 1174 (2004).
26. P. R. Birkin, R. O'Connor, C. Rapple, S. S. Martinez, 'Electrochemical measurement of erosion from individual cavitation events generated from continuous ultrasound', J. Chem. Soc.-Faraday Trans., 94 (22), 3365 (1998).
27. P. R. Birkin, Y. E. Watson, T. G. Leighton, 'Efficient mass transfer from an acoustically oscillated gas bubble', Chem. Commun., (24), 2650 (2001).
28. P. R. Birkin, Y. E. Watson, T. G. Leighton, K. L. Smith, 'Electrochemical detection of faraday waves on the surface of a gas bubble', Langmuir, 18 (6), 2135 (2002).
29. C. J. James, D. E. Mulcahy, B. J. Steel, 'Viscometer calibration standards: viscosities of water between 0 and 60 °C and of selected aqueous sucrose solutions at 25 °C from measurements with a flared capillary viscometer', J. Phys. D: Appl. Phys., 17 (2), 225 (1984).
30. S. J. Konopka, B. McDuffie, 'Diffusion Coefficients Of Ferricyanide And Ferrocyanide Ions In Aqueous Media, Using Twin-Electrode Thin-Layer Electrochemistry', Anal. Chem., 42 (14), 1741 (1970).
31. T. G. Leighton, The Acoustic Bubble, Academic Press Limited, London, 168-172 (1994).
32. D. G. Ramble, A. D. Phelps, T. G. Leighton, 'On the relation between surface waves on a bubble and the subharmonic combination-frequency emission', Acustica, 84 (5), 986 (1998).